



Year: 2014

The protein and contrast agent-specific influence of pathological plasma-protein concentration levels on contrast-enhanced magnetic resonance imaging

Goetschi, Stefan ; Froehlich, Johannes M ; Chuck, Natalie C ; Curcio, Raffaele ; Runge, Val M ; Andreisek, Gustav ; Nanz, Daniel ; Boss, Andreas

Abstract: **OBJECTIVE:** The objective of this study was to measure the protein-specific response of r_1 and r_2 relaxivities of commercially available gadolinium-based magnetic resonance imaging contrast agents to variation of plasma-protein concentrations. **MATERIALS AND METHODS:** In this in vitro study, contrast agent (gadofosveset trisodium, gadoxetate disodium, gadobutrol, and gadoterate meglumine) dilution series (0-2.5 mmol Gd/L) were prepared with plasma-protein (human serum albumin [HSA] and immunoglobulin G [IgG]) concentrations at physiological (42 and 10 g/L HSA and IgG, respectively, Normal) and at 3 pathological levels with HSA/IgG concentrations of 10/10 (solution Alb low), 42/50 (IgG mild), and 42/70 (IgG severe) g/L. Contrast-agent molar relaxivities and relaxivity-enhancing protein-contrast-agent interaction coefficients were determined on the basis of inversion-recovery and spin-echo data acquired at 1.5 and 3.0 T at 37°C. Protein-induced magnetic resonance imaging signal changes were calculated. **RESULTS:** The effective r_1 and r_2 molar relaxivities consistently increased with albumin and IgG concentrations. At 1.5 T, the r_1 values increased by 10.2 (gadofosveset), 4.3 (gadoxetate), 1.3 (gadobutrol), and 1.1 L s mmol (gadoterate), respectively, from the Alb low to the IgG severe solution. At 3.0 T, the r_1 values increased by 2.9 (gadofosveset), 2.3 (gadoxetate), 0.7 (gadobutrol), and 0.9 (gadoterate) L s mmol, respectively. An excess of IgG most strongly increased the r_1 of gadoxetate (+40 and +19% at 1.5 and 3.0 T, respectively, from Normal to IgG severe). An albumin deficiency most strongly decreased the r_1 of gadofosveset (-44% and -20% at 1.5 and 3.0 T, respectively, from Normal to Alb low). The modeling confirmed a strong gadofosveset r_1 enhancement by albumin and suggested stronger IgG than albumin effects on the apparent molar relaxivity of the other agents per protein mass concentration at 1.5 T. **CONCLUSIONS:** Pathological deviations from normal plasma-protein concentrations in aqueous solutions result in changes of effective r_1 and r_2 contrast-agent relaxivities and projected signal enhancements that depend on the contrast agent, the blood-serum protein profile, and the field strength.

DOI: <https://doi.org/10.1097/RLI.0000000000000061>

Posted at the Zurich Open Repository and Archive, University of Zurich

ZORA URL: <https://doi.org/10.5167/uzh-96106>

Journal Article

Published Version

Originally published at:

Goetschi, Stefan; Froehlich, Johannes M; Chuck, Natalie C; Curcio, Raffaele; Runge, Val M; Andreisek, Gustav; Nanz, Daniel; Boss, Andreas (2014). The protein and contrast agent-specific influence of pathological plasma-protein concentration levels on contrast-enhanced magnetic resonance imaging. *Investigative Radiology*, 49(9):608-619.
DOI: <https://doi.org/10.1097/RLI.0000000000000061>

The Protein and Contrast Agent–Specific Influence of Pathological Plasma-Protein Concentration Levels on Contrast-Enhanced Magnetic Resonance Imaging

Stefan Goetschi, MD,* Johannes M. Froehlich, PhD,† Natalie C. Chuck, MD,* Raffaele Curcio, PhD,‡ Val M. Runge, MD,* Gustav Andreisek, MD,* Daniel Nanz, PhD,* and Andreas Boss, MD, PhD*

Objective: The objective of this study was to measure the protein-specific response of r_1 and r_2 relaxivities of commercially available gadolinium-based magnetic resonance imaging contrast agents to variation of plasma-protein concentrations.

Materials and Methods: In this in vitro study, contrast agent (gadofosveset trisodium, gadoxetate disodium, gadobutrol, and gadoterate meglumine) dilution series (0–2.5 mmol Gd/L) were prepared with plasma-protein (human serum albumin [HSA] and immunoglobulin G [IgG]) concentrations at physiological (42 and 10 g/L HSA and IgG, respectively, *Normal*) and at 3 pathological levels with HSA/IgG concentrations of 10/10 (solution *Alb low*), 42/50 (*IgG mild*), and 42/70 (*IgG severe*) g/L. Contrast-agent molar relaxivities and relaxivity-enhancing protein–contrast-agent interaction coefficients were determined on the basis of inversion-recovery and spin-echo data acquired at 1.5 and 3.0 T at 37°C. Protein-induced magnetic resonance imaging signal changes were calculated.

Results: The effective r_1 and r_2 molar relaxivities consistently increased with albumin and IgG concentrations. At 1.5 T, the r_1 values increased by 10.2 (gadofosveset), 4.3 (gadoxetate), 1.3 (gadobutrol), and 1.1 L s^{−1} mmol^{−1} (gadoterate), respectively, from the *Alb low* to the *IgG severe* solution. At 3.0 T, the r_1 values increased by 2.9 (gadofosveset), 2.3 (gadoxetate), 0.7 (gadobutrol), and 0.9 (gadoterate) L s^{−1} mmol^{−1}, respectively. An excess of IgG most strongly increased the r_1 of gadoxetate (+40 and +19% at 1.5 and 3.0 T, respectively, from *Normal* to *IgG severe*). An albumin deficiency most strongly decreased the r_1 of gadofosveset (−44% and −20% at 1.5 and 3.0 T, respectively, from *Normal* to *Alb low*). The modeling confirmed a strong gadofosveset r_1 enhancement by albumin and suggested stronger IgG than albumin effects on the apparent molar relaxivity of the other agents per protein mass concentration at 1.5 T.

Conclusions: Pathological deviations from normal plasma-protein concentrations in aqueous solutions result in changes of effective r_1 and r_2 contrast-agent relaxivities and projected signal enhancements that depend on the contrast agent, the blood-serum protein profile, and the field strength.

Key Words: contrast-enhanced MR imaging, gadolinium-based contrast agents, contrast-agent relaxivity, relaxometry, human blood serum proteins

(*Invest Radiol* 2014;49: 608–619)

Received for publication November 22, 2013; and accepted for publication, after revision, February 24, 2014.

From the *Institute for Diagnostic and Interventional Radiology, University Hospital Zürich; †Institute of Pharmaceutical Sciences, Swiss Federal Institute of Technology, ETHZ; and ‡Institute of Clinical Chemistry, University Hospital Zürich, Zürich, Switzerland.

Presented in part as a conference abstract at the Annual Meeting of the International Society for Magnetic Resonance in Medicine, May 10–16, 2014, Milano, Italy.

Conflict of interest and sources of funding: Immunoglobulin G and albumin parent solutions were generously provided by CSL Behring (Bern, Switzerland). CSL Behring did not have an influence on the study design, the scientific evaluation, or on the report of the data.

Supplemental digital contents are available for this article. Direct URL citations appear in the printed text and are provided in the HTML and PDF versions of this article on the journal's Web site (www.investigativeradiology.com)

Reprints: Daniel Nanz, PhD, Institut für Diagnostische und Interventionelle Radiologie, Universitätsspital Zürich, Rämistrasse 100, 8091 Zürich. E-mail: daniel.nanz@usz.ch.

Copyright © 2014 by Lippincott Williams & Wilkins
ISSN: 0020-9996/14/4909-0608

Gadolinium-based magnetic-resonance (MR) contrast agents (GBCAs) are administered in a large number of clinical examinations worldwide.¹ They provide morphological and functional information in a broad range of clinical settings by shortening recovery times T_1 and T_2 of longitudinal and transverse water magnetization in their close proximity, which can be exploited to depict corresponding regions with increased or reduced signal intensity, respectively.

The effect strength, with which a contrast agent changes relaxation times and MR imaging signal intensities, is quantitatively given by its longitudinal and transverse molar relaxivities, r_1 and r_2 , respectively.²

It is well known that GBCA relaxivities depend on concentration of proteins, such as human serum albumin (HSA).^{3–6} Some agents were specifically designed to strongly interact with albumin to increase their effective relaxivity in blood and other body fluids.^{7–9} Therefore, it seems likely that pathological deviations from normal protein concentrations cause signal changes in contrast-enhanced MR imaging. It is not clear though whether such effects could be large enough to impact diagnoses, given a sufficiently unusual combination of contrast medium, image acquisition, data evaluation, and pathological protein profile.

The objectives of our study were to quantitatively measure effective r_1 and r_2 molar relaxivities of 4 commonly used commercially available GBCAs in sodium-chloride solutions and in the presence of physiologically and pathologically abnormal plasma-protein (HSA and γ -immunoglobulin G [IgG]) concentrations at 2 field strengths and to use these values to project the expected signal response for some commonly used MR imaging pulse sequences.

MATERIALS AND METHODS

Dilution Series

Stabilized solutions of human albumin and human IgG (20% each, CSL Behring, Bern, Switzerland) were mixed with sterile 0.9% aqueous sodium chloride to produce 5 protein stock solutions at varying protein concentration: *Normal* solution, 42 g/L of albumin and 10 g/L of IgG; *Alb low*, 10/10; *IgG mild*, 42/50; *IgG severe*, 42/70 g/L; *NaCl only*, 0/0.

Contrast media solutions at 0.25 mol Gd/L were obtained, where required after dilution with aqueous sodium chloride: that of gadofosveset trisodium (0.25 mol/L, Ablavar; Lantheus Medical Imaging, N. Billerica, MA), that of gadoxetate disodium (0.25 mol/L, Primovist; Bayer Healthcare, Leverkusen, Germany), gadobutrol (1 mol/L, Gadovist; Bayer Healthcare), and that of gadoterate meglumine (0.5 mol/L, Dotarem; Guerbet AG, Roissy, France), and diluted with protein stock solutions to obtain dilution-series stock solutions at 12.5 mmol Gd/L.

Repeatedly, an aliquot of 0.6 mL of the dilution-series solution at the current dilution step was diluted with 2.4 mL of the corresponding protein stock solution to reach gadolinium concentrations of 2.5, 0.5, 0.1, 0.02, and 0.004 mmol Gd/L, respectively. The dilution series were independently prepared twice. A total of 240 samples in 2-mL plastic

vials were, in turn, collected in a rack that was inserted in a temperature-controlled water-tank phantom for imaging (Fig. 1).

Laboratory Analyses

The total protein concentration of the protein solutions was determined by the Biuret reaction¹⁰ on a Cobas Integra 800 analyzer (Roche Diagnostics, Basel, Switzerland). Protein electrophoresis was performed on an alkaline-buffered (pH, 8.6) agarose gel (Sebia Hydragel Protein(E) K20, Sebia, Lisses, France), applying a voltage of 90 V for 18 minutes. Immediately after the electrophoresis, the fractionated proteins were fixed (60% ethanol, 10% acetic acid, and 30% deionized water) and stained with amido black solution for 4 minutes. The excess of stain was removed from the gel by 3 successive baths of an acidic destaining solution (pH, 2). The gel was dried, and electrophoresis curves were obtained by densitometric scanning of the dried gel.

MR Imaging and Determination of Relaxation Rates

Data were acquired in clinical whole-body MR scanners operating at 1.5 and 3.0 T (Signa HDxt and Discovery MR750, respectively; GE Healthcare, Waukesha, WI) using transmit-receive “QUADKNEE” knee coils. During image acquisition, the water phantom was kept at a constant temperature of 37°C with water circulating through a temperature-controlled bath.

Longitudinal Relaxation Rates, R_1

Two-dimensional inversion-recovery fast-spin-echo images were acquired with varying inversion times (TIs) and constant pre-scan parameters. Parameters at 1.5 T are as follows: echo time (TE), 6.3 milliseconds; repetition time (TR), 6000 milliseconds; echo-train length, 2; receive bandwidth (RBW), ± 41.7 kHz; matrix size, 256×512 ; in-plane voxel dimensions, 0.39×0.39 mm; slice thickness (THK), 8 mm; and TIs of 50, 60, 80, 100, 120, 140, 180, 200, 400, 600, 1000, 1500, 2000, and 3000 milliseconds. Parameters at 3.0 T are as follows: TE, 10.4 milliseconds; TR, 6000 milliseconds; echo-train length, 2; RBW, ± 15.6 kHz; matrix size, 128×256 ; in-plane voxel dimension, 0.78×0.78 mm; THK, 8 mm; TI, as those on the 1.5-T scanner. T_1 constants were obtained from fits of the expression $S0 \times (1 - 2 \times \text{Exp}(-TI/T_1))$ to

the experimental data, using custom MATLAB (MathWorks, Natick, MA) code. R_1 rates were obtained as $1/T_1$. T_1 values shorter than 80 milliseconds and longer than 5 seconds were excluded from further analyses. This led to an exclusion of mostly data points of the protein-binding contrast agents gadovosfiset and gadoxetate at the highest concentration, that is, 2.5 mM, at both field strengths. The total number of data points in each fit is listed in Table 2.

Transverse Relaxation Rates, R_2

Two-dimensional spin-echo images were acquired with varying TEs and constant pre-scan parameters. Parameters at both field strengths are as follows: TR, 7500 milliseconds; RBW, ± 15.6 kHz; matrix size, 192×256 ; in-plane voxel dimensions, 0.78×0.78 mm; THK, 8 mm; and TE times of 20, 50, 100, 400, and 800 milliseconds. T_2 constants were obtained from fits of the expression $S0 \times \text{Exp}(-TE/T_2) + N$ to the experimental data, as above for T_1 constants. T_2 values shorter than 20 milliseconds and longer than 5 seconds were excluded from further analyses. R_2 rates were obtained as $1/T_2$. For the *NaCl only* solutions, without proteins, this led to the exclusion of some data points at one or more of the 3 lowest gadolinium concentrations (0–0.02 mM), whereas, for the protein solutions, it tended to exclude data points at the 2 highest contrast-agent concentrations, particularly so for the protein-binding contrast agents. The total number of data points in each fit is listed in Table 2.

Contrast-Agent Relaxivities

The apparent or effective molar relaxivities, r_1^{eff} , r_2^{eff} , at a given protein concentration, were estimated from the relaxation rates $R_{1,2}(c)$ measured at different contrast-agent concentrations, c , according to equation [1], by linear regression. These data served as reference during the evaluation and are not shown. The reported effective molar relaxivities were obtained from the results of fits of equation [2], as detailed below.

$$\begin{aligned} R_1(c) &= R_1^{pre} + r_1^{eff} * c, \\ R_2(c) &= R_2^{pre} + r_2^{eff} * c, \end{aligned} \quad [1]$$

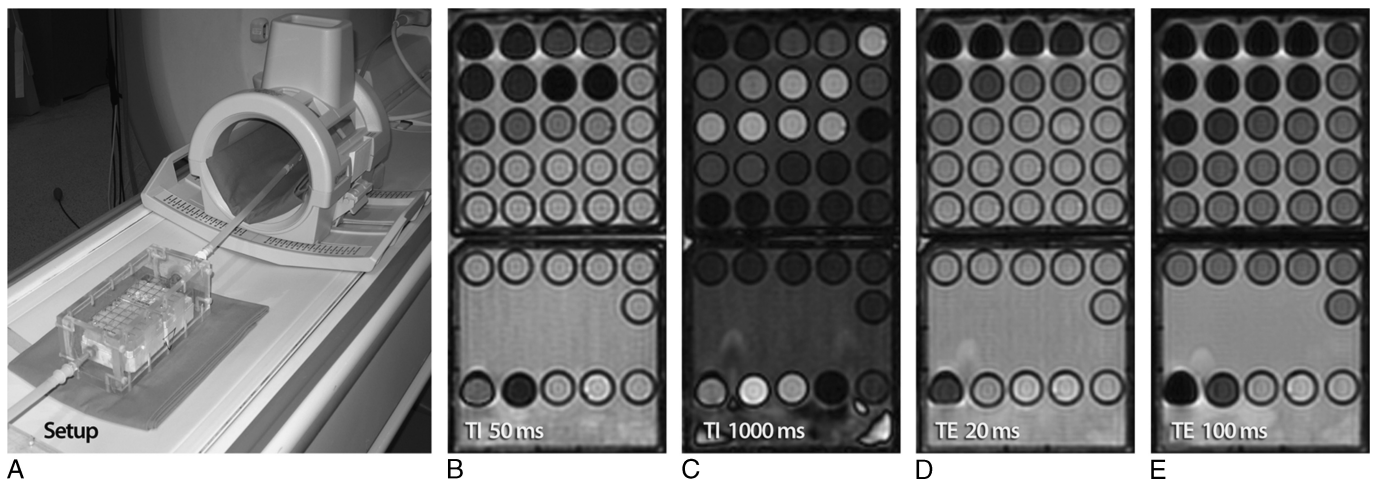


FIGURE 1. A, The experimental setup with the acrylic water-tank phantom that was attached to plastic tubes circulating 37°C water from a thermo-regulated water bath outside the scanner room. The phantom was sealed during the experiments with an acrylic cover attached with plastic screws. B to E, Representative MR images: B and C, Inversion recovery fast spin-echo images at TI of 50 and 1000 milliseconds, respectively. D and E, Spin-echo images at TE of 20 and 100 milliseconds, respectively. Contrast-agent concentrations decrease from the vials in the upper parts of the pictures to the lower part. The lowest row of vials contains solutions of the control series without serum proteins. Slight Gibbs' ringing artifacts may be noted at interfaces with high signal-intensity changes.

Relaxivity-Enhancement Model

The effective molar relaxivities, $r_{1,2}^{eff}$, and pre-contrast relaxation rates $R_{1,2}^{pre}$ in equation [1] depend on protein concentrations.³⁻⁹ A more general signal equation should take that into consideration. Thus, pooled relaxation rates of a contrast-agent dilution series at a given field strength, at all protein concentrations levels and from both dilution series, were fitted by least-square linear regression to the following expressions:

$$\begin{aligned} R_1(c, c^{HSA}, c^{IgG}) &= R_{10}^{pre} + r_1^{HSA} c^{HSA} + r_1^{IgG} c^{IgG} + (r_1^{H_2O} + r_1^{HSA} c^{HSA} + r_1^{IgG} c^{IgG})c, \\ R_2(c, c^{HSA}, c^{IgG}) &= R_{20}^{pre} + r_2^{HSA} c^{HSA} + r_2^{IgG} c^{IgG} + (r_2^{H_2O} + r_2^{HSA} c^{HSA} + r_2^{IgG} c^{IgG})c, \end{aligned} \quad [2]$$

where c is the contrast-agent concentration and c^{HSA} and c^{IgG} are albumin and IgG concentrations, respectively. Equation [2] expands the relaxivities from equation [1] according to the following:

$$\begin{aligned} r_1^{eff} &= r_1^{H_2O} + r_1^{HSA} c^{HSA} + r_1^{IgG} c^{IgG}, \\ r_2^{eff} &= r_2^{H_2O} + r_2^{HSA} c^{HSA} + r_2^{IgG} c^{IgG}, \end{aligned} \quad [3]$$

with the “zero-protein contrast-agent relaxivities,” $r_{1,2}^{HSA}$, $r_{1,2}^{IgG}$, and the relaxivity-enhancement coefficients $re_{1,2}^{HSA,IgG}$. Equation [2] expands the pre-contrast relaxation rates from equation [1] according to the following:

$$\begin{aligned} R_1^{pre} &= R_{10}^{pre} + r_1^{HSA} c^{HSA} + r_1^{IgG} c^{IgG} \\ R_2^{pre} &= R_{20}^{pre} + r_2^{HSA} c^{HSA} + r_2^{IgG} c^{IgG}, \end{aligned} \quad [4]$$

with the protein relaxivities $r_{1,2}^{HSA}$ and $r_{1,2}^{IgG}$ and the “zero protein, pre-contrast relaxation rates” $R_{10,20}$.

When setting both protein concentrations to zero, equation [2] takes on the form of equation [1]. Equation [2] allows all data points for a given combination of field strength and contrast agent to be considered in a single fit, which resulted in an improved numerical fit stability, compared with repeated isolated fits of equation [1] to partial data. It also allows a phenomenological differentiation of protein-specific effects on both native relaxation rates and on contrast-agent molar relaxivity values. Finally, it allows straightforward interpolation and extrapolation compatible with our results to other protein concentrations.

Equation [2] still assumes a linear relationship between relaxation rates and gadolinium concentration, which is known to not always be correct. Nevertheless, we chose to work with equation [2] to keep the model simple and the number of fitted variables as small as possible, avoiding an “overfitting” of the data, and to be able to discuss the results for the different contrast agents in a single approximate model that has been used in a large body of previous literature. Compare the Results and Discussions sections for corresponding limitations. The fits of equation [2] to experimental relaxation rates were done with custom Python routines (Python Software Foundation, Beaverton, OR) based on scikit-learn.¹¹

Simulated Effects on MR Imaging Signal

Signal-intensity profiles were calculated for the following 1.5-T MR imaging sequences with custom MATLAB routines:

- MR angiographic blood-pool T1-weighted spoiled gradient-echo signal, as $(\sin\theta (1 - E_1) E_2) / (1 - \cos\theta E_1)$; $E_1 = \exp(-TR/R_1)$, and $E_2 = \exp(-TE/R_2)$, $TR = 3.4$ milliseconds, $TE = 1.4$ milliseconds, $\theta = 25$ degrees.
- Tissue T1-weighted spin-echo signal, as $(1 - E_1) E_2$; $TR = 500$ milliseconds, $TE = 10$ milliseconds.
- Tissue T2-weighted spin echo signal, as $(1 - E_1) E_2$; $TR = 6000$ milliseconds, $TE = 100$ milliseconds.
- Generic tissue T2-weighted sequence signal, as in, for example, dynamic-susceptibility contrast MRI, as $(1 - E_1) E_2$; $TR = 2000$ milliseconds, $TE = 50$ milliseconds.

For (a) blood, relaxation times T_1 and T_2 of 1441 and 327 milliseconds¹² were used; for (b) to (d) “tissue” T_1 and T_2 of 1000 and 100 milliseconds.

Statistical Analysis

Squared linear regression coefficients and root mean squared errors were calculated for all fits. Plots of fit-residuals versus experimental relaxivity values were checked for systematic deviations. The 90% confidence interval limits for the results of the relaxivity-modeling fits were estimated by the bootstrap method.¹³

RESULTS

Laboratory Analyses

The differences between measured minus targeted protein concentrations were between 1% and 5% and, thus, not significant, considering the coefficient of variation of the used laboratory method of 2.5%. Electrophoresis curves are displayed in Figure 2. Qualitatively, the relative amounts of the albumin and the γ -globulin fractions from electrophoresis were consistent with the targeted physiological situation (*Normal*), hypoalbuminemia (*Alb low*), as well as mild (*IgG mild*) and severe (*IgG severe*) gammopathy, respectively.

Relaxation Rates

Sample images used for the relaxation-rate determinations are shown in Figure 1. Representative data points and exponential fits are shown in Figure 3. Figure 4 displays plots of relaxation-rate enhancements versus gadolinium concentration as observed for all contrast agents in the *Normal* protein-content solutions of dilution series 1. Figure 5 shows plots of relaxation-rate enhancements versus gadolinium concentration as observed for gadofosveset in the solutions with different protein contents in dilution series 1. Both axes in Figures 4 and 5 have a logarithmic scaling to emphasize deviations from a linear dependence of the gadolinium concentration. Such deviations were particularly prominent for transverse relaxation and the protein-binding contrast agents, whereas the linear model approximated enhancement of longitudinal relaxation within the concentration range of interest well.

Relaxivity-Enhancement Fits

Results from the pooled fits of equation [2] are summarized in Tables 1 and 2, compared below for more details. Plots of residuals versus average of experimental and fit data for all fits (see Supplemental Figure 1, Supplemental Digital Content 1, <http://links.lww.com/RLI/A149>) and, specifically, for the fits of gadofosveset (see Supplemental Figure 2 [Supplemental Digital Content 2, <http://links.lww.com/RLI/A150>], Supplemental Figure 3 [Supplemental Digital Content 3, <http://links.lww.com/RLI/A151>], Supplemental Figure 4 [Supplemental Digital Content 4, <http://links.lww.com/RLI/A152>], and Supplemental Figure 5 [Supplemental Digital Content 5, <http://links.lww.com/RLI/A153>]) did not reveal major overall systematic deviations.

Contrast-Agent Relaxivities

The effective molar relaxivities at a given protein concentration, as defined by equation [1], are listed in Table 1 and graphically visualized in Figure 6. These values were calculated from the fit results shown in Table 2, with the formula given in equation [3]. At low total protein concentrations (*NaCl only*, *Alb low*, and *Normal*), the 3.0-T r_1^{eff} and r_2^{eff} relaxivities were slightly higher than the corresponding 1.5-T values, whereas, at higher protein concentrations (*IgG mild* and *IgG severe*), the opposite was observed. The same behavior was also observed in direct fits of single dilution-series data at a given protein concentration.

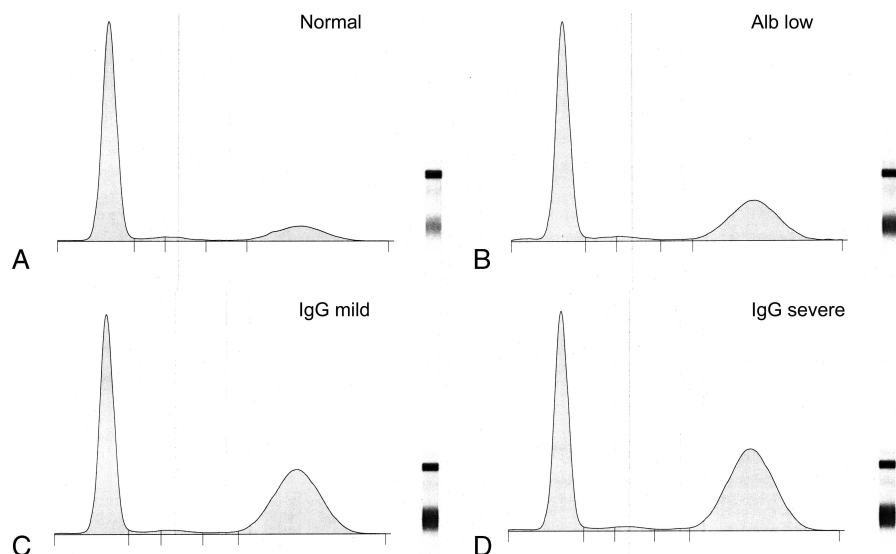


FIGURE 2. Densitogram of the electrophoresis of the 4 solutions with varying serum protein content: *physiological (Normal)* solution (A) and the solutions mimicking hypoalbuminemia (*Alb low*, different scaling than in A) (B) as well as mild (*IgG mild*) (C), and severe (*IgG severe*) gammopathy (D). Note the absence of α - and β -globulin components from all solutions (A-D).

Protein-Induced Changes of Contrast-Agent Relaxivities

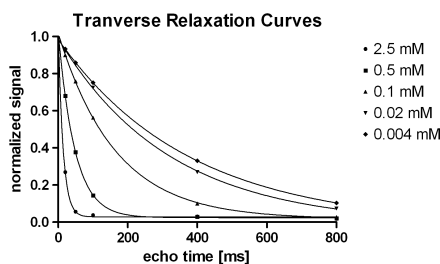
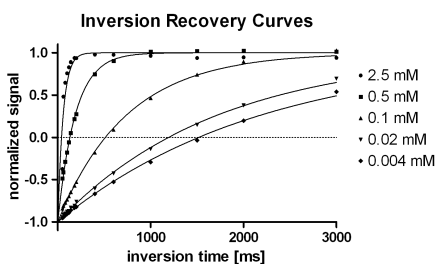
Absolute and relative relaxivity changes from *Normal* to pathology-mimicking protein solutions are also summarized in Table 1. In general, higher protein content correlated with increased r_1 and r_2 relaxivities and lower protein content correlated with decreased r_1 and r_2 relaxivities. The largest decreases versus the *Normal* solutions were found for the *NaCl only* solution, that is, upon removal of physiological amounts of albumin and IgG. The largest relative negative changes were found for gadofosveset. Negative changes were also

found for the hypoalbuminemia solution *Alb low*. In contrast, positive changes were observed for both mild and severe gammopathy solutions *IgG mild* and *IgG severe*. The largest relative positive changes were observed for gadodotatate.

Protein-Specific Relaxivity Enhancement

Large contrast-agent relaxivity-enhancing coefficients re_1^{HSA} and re_2^{HSA} that were significantly larger than corresponding coefficients re_1^{IgG} and re_2^{IgG} were found for gadofosveset (Table 2). In contrast, in most cases for the other contrast agents, the corresponding

Gadofosveset



Gadoterate

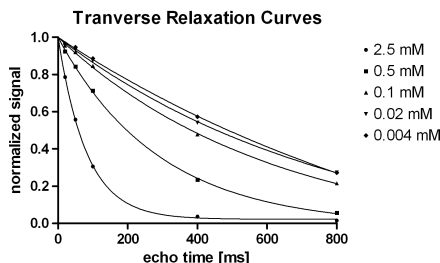
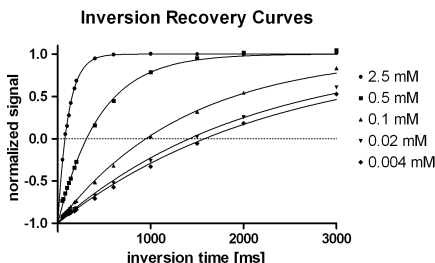


FIGURE 3. Exemplary inversion-recovery curves (R_1 quantification) and transverse relaxation curves (R_2 quantification) from the first dilution series at 3 T of gadofosveset and gadoterate, *Normal* solution.

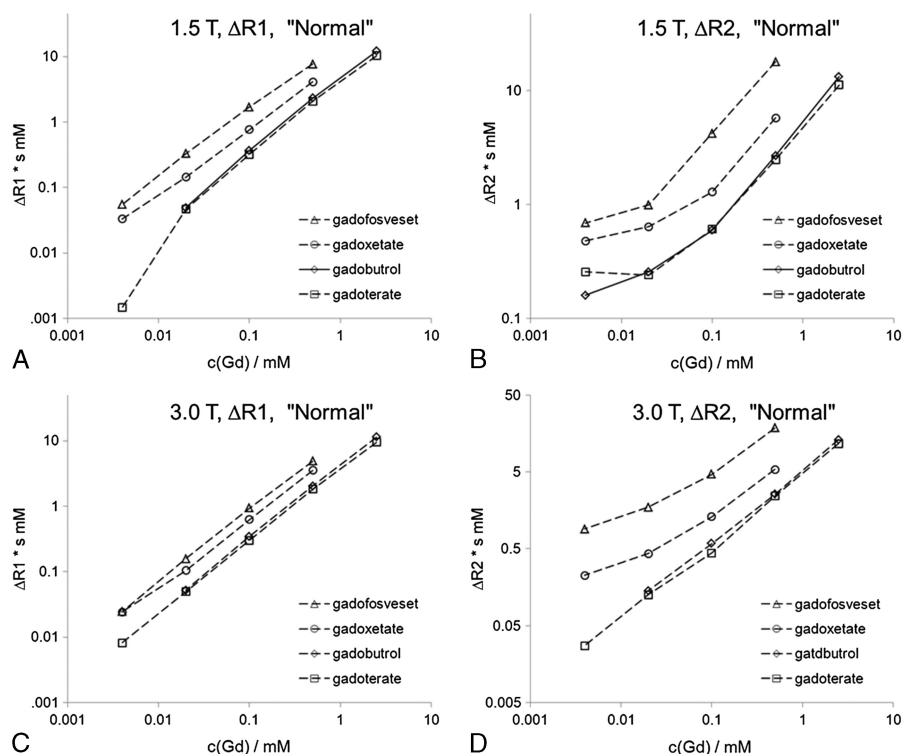


FIGURE 4. Relaxation-rate changes induced by the 4 contrast agents at *physiological* albumin and IgG content, that is, in the *Normal* solutions of dilution series 1; $\Delta R1$ (A, C) and $\Delta R2$ (B, D) values at 1.5 T (A, B) and at 3.0 T (C, D), respectively.

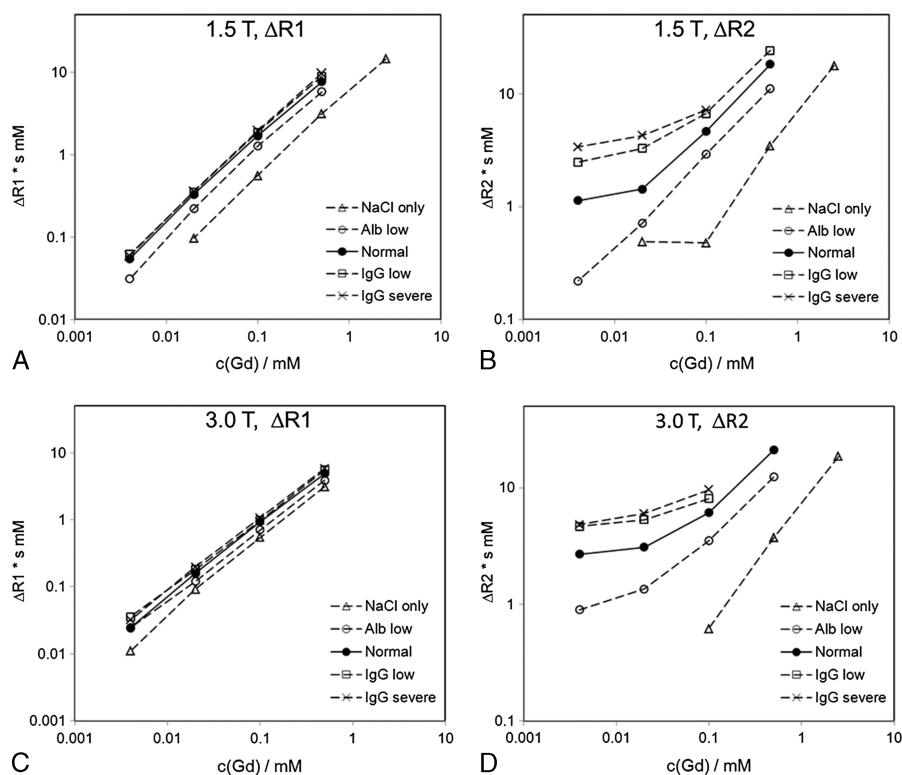


FIGURE 5. Relaxation-rate changes induced by gadofosveset as observed in dilution series 1; $\Delta R1$ (A, C) and $\Delta R2$ (B, D) values at 1.5 T (A, B) and at 3.0 T (C, D), respectively.

TABLE 1. Effective Longitudinal and Transverse Molar Relaxivities of 4 Contrast Media at Varying Protein Concentration and Field Strength

B0 = 1.5 T						B0 = 3.0 T					
	Gadofosveset	Gadoxetate	Gadobutrol	Gadoterate	Gadofosveset	Gadoxetate	Gadobutrol	Gadoterate		Gadobutrol	Gadoterate
Longitudinal $r_{1\rho}^{eff}$											
NaCl only	5.91 (-9.36/-61) [5.75-8.26]	5.36 (-2.22/-29) [5.30-5.50]	3.56 (-0.65/-16) [3.37-3.62]	3.31 (-0.40/-11) [3.22-3.45]	6.95 (-2.71/-28) [6.25-7.43]	5.70 (-1.49/-21) [5.24-6.15]	3.72 (-0.67/-15) [3.40-4.03]	3.46 (-0.48/-12) [3.10-3.81]			
Alb low	8.58 (-6.69/-44) [7.57-9.64]	6.27 (-1.31/-17) [5.80-6.36]	3.84 (-0.38/-9) [3.76-3.96]	3.53 (-0.19/-5) [3.46-3.64]	7.71 (-1.95/-20) [7.16-8.07]	6.23 (-0.96/-13) [5.85-6.57]	3.91 (-0.48/-11) [3.64-4.15]	3.65 (-0.29/-7) [3.37-3.92]			
Normal	15.27 (0.00/0) [9.67-15.77]	7.60 (0.00/0) [6.92-8.30]	4.22 (0.00/0) [3.6-4.84]	3.72 (0.00/0) [3.37-4.10]	9.66 (0.00/0) [5.59-9.89]	7.17 (0.00/0) [7.09-8.24]	4.38 (0.00/0) [4.17-4.56]	3.93 (0.00/0) [3.75-4.11]			
IgG mild	17.61 (2.32/+15) [15.52-18.64]	9.60 (+2.00/+26) [9.40-9.84]	4.84 (+0.60/+14) [4.55-5.08]	4.34 (+0.60/+16) [4.26-4.49]	10.28 (+0.60/+6) [9.26-11.06]	8.09 (+0.92/+13) [7.63-8.28]	4.53 (0.16/+4) [3.89-4.85]	4.34 (+0.40/+10) [4.20-4.44]			
IgG severe	18.78 (+3.48/+23) [14.79-19.70]	10.58 (+3.00/+40) [9.30-11.67]	5.14 (+0.90/+21) [4.46-5.42]	4.64 (+0.90/+24) [4.38-4.70]	10.58 (+0.90/+9) [9.30-11.67]	8.55 (+1.38/+19) [8.06-8.87]	4.60 (0.24/+5) [3.31-5.00]	4.54 (+0.60/+15) [4.35-4.72]			
Transverse $r_{2\rho}^{eff}$											
NaCl only	7.15 (-27.59/-79) [6.77-7.41]	6.44 (-2.96/-31) [5.95-6.58]	4.03 (-0.88/-18) [3.64-4.27]	3.86 (-0.62/-14) [3.64-4.03]	7.56 (-29.55/-80) [7.01-8.15]	6.63 (-3.82/-37) [6.35-6.96]	4.11 (-1.39/-25) [3.48-4.31]	3.89 (-0.72/-16) [3.58-4.18]			
Alb low	14.61 (-20.13/-58) [13.35-16.25]	8.18 (-1.22/-13) [7.84-8.35]	4.63 (-0.29/-6) [4.37-4.87]	4.30 (-0.19/-4) [4.14-4.45]	14.93 (-22.18/-60) [13.48-17.99]	8.69 (-1.76/-17) [8.55-9.04]	4.67 (-0.83/-15) [4.18-4.86]	4.32 (-0.29/-6) [4.07-4.55]			
Normal	34.74 (0.00/0) [33.49-41.48]	9.38 (0.00/0) [7.35-10.22]	4.92 (0.00/0) [4.18-5.36]	4.51 (0.00/0) [4.41-5.78]	37.11 (0.00/0) [35.38-41.81]	10.44 (0.00/0) [9.22-11.59]	5.51 (0.00/0) [5.18-6.51]	4.62 (0.00/0) [4.55-5.48]			
IgG mild	39.42 (4.68/+13) [33.40-46.24]	14.81 (+5.44/+58) [13.92-15.29]	6.93 (+2.00/+41) [6.45-7.63]	5.98 (+1.48/+33) [5.52-6.17]	38.87 (+1.76/+5) [35.60-55.86]	16.48 (+6.04/+58) [15.93-17.04]	6.72 (+1.20/+22) [6.13-7.04]	5.98 (+1.36/+30) [5.52-6.17]			
IgG severe	41.76 (7.02/+20) [31.94-53.54]	17.52 (+8.16/+87) [16.42-18.28]	7.93 (3.00/+61) [7.05-8.99]	6.75 (+2.22/+50) [6.31-7.16]	39.74 (+2.64/+7) [32.21-64.89]	19.50 (+9.06/+87) [18.26-20.18]	7.32 (+1.80/+33) [6.83-7.93]	6.66 (+2.04/+44) [6.33-7.04]			

Absolute and relative (in percentage) changes from the solution with *Normal* protein concentrations are given in parentheses.
Low and high limits of 90% confidence intervals are given in brackets.
Bold values indicates the most important effective molar relaxivity.
Alb indicates albumin; IgG, immunoglobulin G; NaCl, sodium chloride.

TABLE 2. Longitudinal and Transverse Relaxivity Parameters of 4 Contrast Media, Albumin, and IgG at 1.5 and 3 T

	B0 = 1.5 T				B0 = 3.0 T			
	Gadofosveset	Gadoxetate	Gadobutrol	Gadoterate	Gadofosveset	Gadoxetate	Gadobutrol	Gadoterate
Longitudinal								
$r_{1H_2O}^*$	5.91 [5.75–8.26]	5.36 [5.30–5.50]	3.56 [3.37–3.62]	3.31 [3.22–3.45]	6.95 [6.25–7.43]	5.70 [5.24–6.15]	3.72 [3.40–4.03]	3.46 [3.10–3.81]
re_{1HSA}^\dagger	209 [152–516]	41 [21–62]	12 [(-7)–32]	6 [(-5)–19]	61 [11–80]	30 [17–47]	15 [4–27]	9 [(-2)–20]
re_{1IgG}^\ddagger	58 [(-16)–76]	50 [35–63]	15 [(-1)–31]	15 [7–22]	15 [(-8)–55]	23 [5–30]	4 [(-13)–12]	10 [4–16]
r_{1HSA}^\S	-3 [(-18)–2]	1 [(-1)–2]	1 [(-2)–4]	1 [0–4]	1 [0–2]	0 [0–1]	0 [(-2)–2]	0 [(-1)–2]
r_{1IgG}^\P	1 [0–3]	2 [1–3]	2 [1–3]	2 [1–5]	2 [0–2]	2 [1–3]	3 [2–5]	3 [2–5]
re_{1HSA}/re_{1IgG}	3.6	0.8	0.8	0.4	4.1	1.3	3.8	0.9
Range $c(Gd)$ §	0.0–2.5	0.0–2.5	0.0–2.5	0.0–2.5	0.0–0.5	0.0–0.5	0.0–2.5	0.0–2.5
No. data points ¶	50	51	56	60	50	50	57	60
r^2 ¶¶	0.987	0.999	0.990	0.997	0.990	0.997	0.995	0.995
$r_{mse}\#$	4.19	2.87	3.56	4.37	2.36	1.92	3.94	4.42
Transverse								
$r_{2H_2O}^*$	7.15 [6.77–7.41]	6.44 [5.95–6.58]	4.03 [3.64–4.27]	3.86 [3.64–4.03]	7.56 [7.01–8.15]	6.63 [6.35–6.96]	4.11 [3.48–4.31]	3.89 [3.58–4.18]
re_{2HSA}^\dagger	629 [533–1040]	38 [(-23)–61]	9 [(-20)–25]	6 [1–31]	693 [604–1872]	55 [15–91]	26 [14–59]	9 [1–25]
re_{2IgG}^\ddagger	117 [(-200)–340]	136 [111–155]	50 [31–87]	37 [21–46]	44 [(-316)–454]	151 [115–180]	30 [2–45]	34 [20–42]
r_{2HSA}^\S	3 [(-22)–15]	22 [18–29]	14 [10–19]	14 [10–17]	23 [(-13)–35]	35 [28–43]	22 [18–26]	23 [19–28]
r_{2IgG}^\P	40 [33–49]	43 [39–46]	43 [39–46]	46 [44–48]	52 [44–71]	52 [47–57]	59 [55–62]	59 [55–62]
re_{2HSA}/re_{2IgG}	5.4	0.3	0.2	0.2	16	0.4	0.9	0.9
Range $c(Gd)$ §	0.0–2.5	0.0–2.5	0.0–2.5	0.0–2.5	0.0–2.5	0.0–2.5	0.0–2.5	0.0–2.5
No. data points	50	49	54	54	42	45	54	55
r^2 ¶¶	0.978	0.998	0.990	0.997	0.977	0.996	0.995	0.994
$r_{mse}\#$	8.33	7.73	7.78	7.05	8.78	7.16	7.72	7.16

Low and high limits of 90% confidence intervals for each parameter are given in brackets.
*Contrast-agent relaxivity in aqueous sodium chloride solution, in units of $L\ s^{-1}\ mmol^{-1}$.
†Protein-specific relaxivity enhancement due to contrast-agent-protein interaction, in units of $L^2s^{-1}\ mmol^{-1}\ kg^{-1}$.
‡Protein-specific relaxivity, also affecting pre-contrast relaxation rates, in units of $L\ s^{-1}\ kg^{-1}$.
§Minimum to maximum gadolinium concentration range of data points in the fit, in units of $mmol\ L^{-1}$.
||Number of experimental relaxation-rate values fitted in the fit; maximum of 60 (6 contrast-agent concentrations, 5 different protein contents, 2 independent series).
¶Squared linear regression coefficient, fits of equation [2].
#Root of mean squared error, in units of s^{-1} , fits of equation [2].
Bold values indicates the primary fit-result data.
H₂O indicates water; HSA, human serum albumin; IgG, immunoglobulin G.

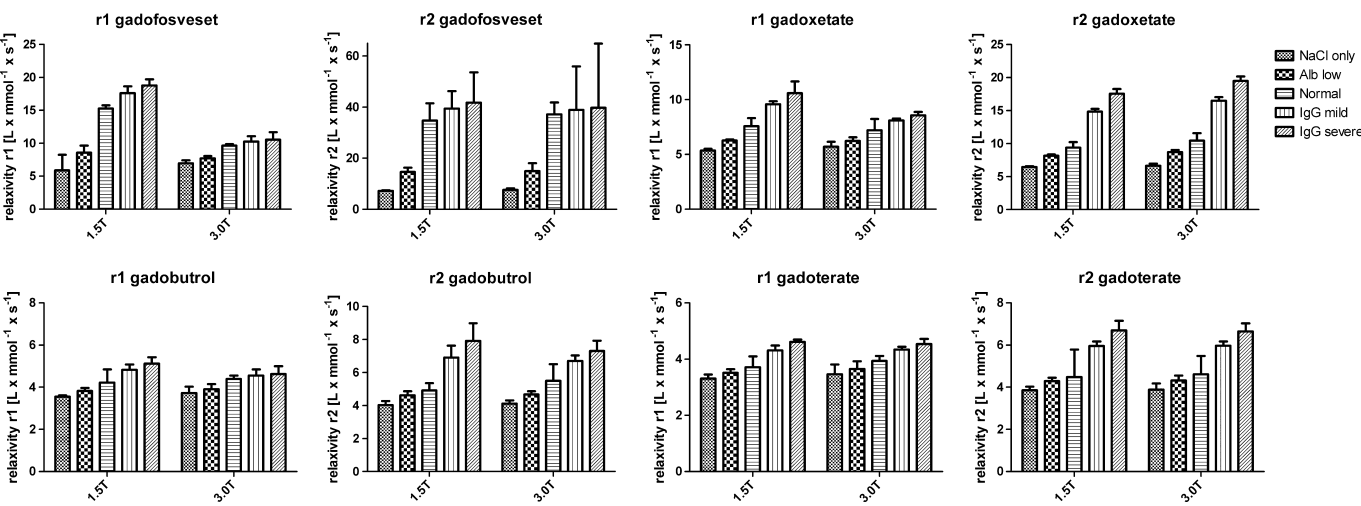


FIGURE 6. Graphical representation of effective molar relaxivities r_1 and r_2 of 4 GBCAs at magnetic field strengths of 1.5 T and 3.0 T at varying serum-protein content, compare Table 1 for numerical values. Note the different ordinate scales. Error bars indicate 90% confidence intervals.

IgG coefficients were at least as large as the albumin coefficients, particularly those describing transverse relaxation effects, re_2^{IgG} .

absence of any contrast agent. Immunoglobulin G had a larger influence than did albumin.

Protein Relaxivity

The coefficients assessing direct effects of the proteins on longitudinal relaxation, $r_1^{HSA,IgG}$, were negligibly small at both field strengths (Table 2). In contrast, $r_2^{HSA,IgG}$ values indicated a direct influence of both proteins on transverse relaxation rates, even in the

Simulated Effects on MR Imaging Signal

Simulated signal curves for common MR imaging sequences are shown in Figures 7 to 10. The gadofosveset-induced signal change strongly depended on the albumin level for all sequences, whereas the influence of IgG was noticeably smaller. In distinction,

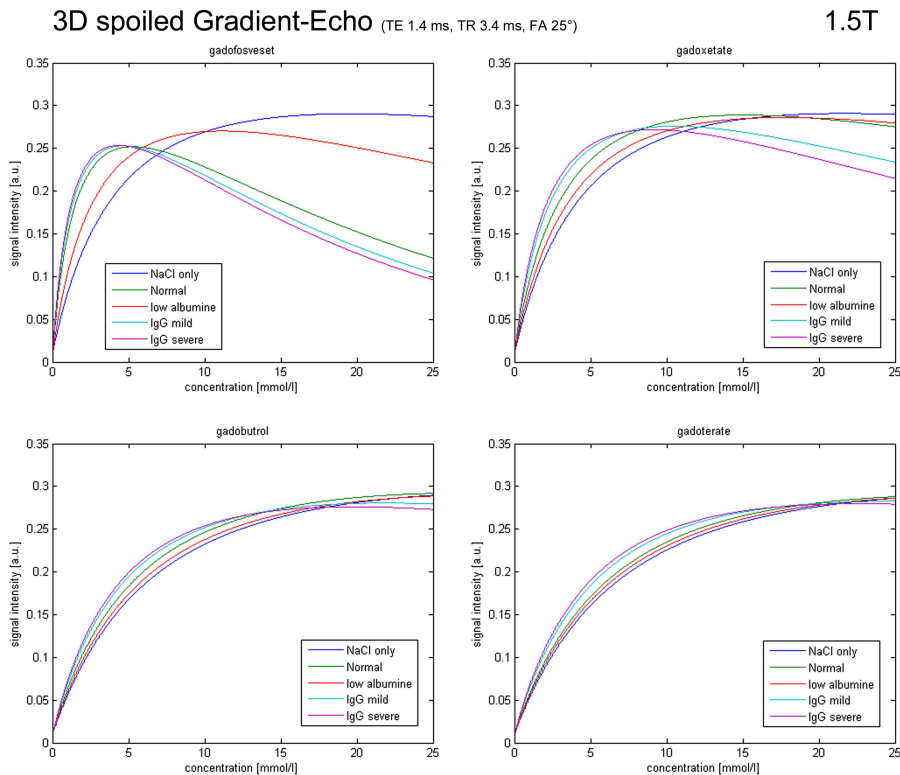


FIGURE 7. Simulated MR angiography signal as a function of the contrast-medium and human serum-protein concentrations (TR/TE/flip angle, 3.4 milliseconds/1.4 milliseconds/25 degrees; precontrast, 1.5 T (blood) T1/T2, 1441/327 milliseconds).

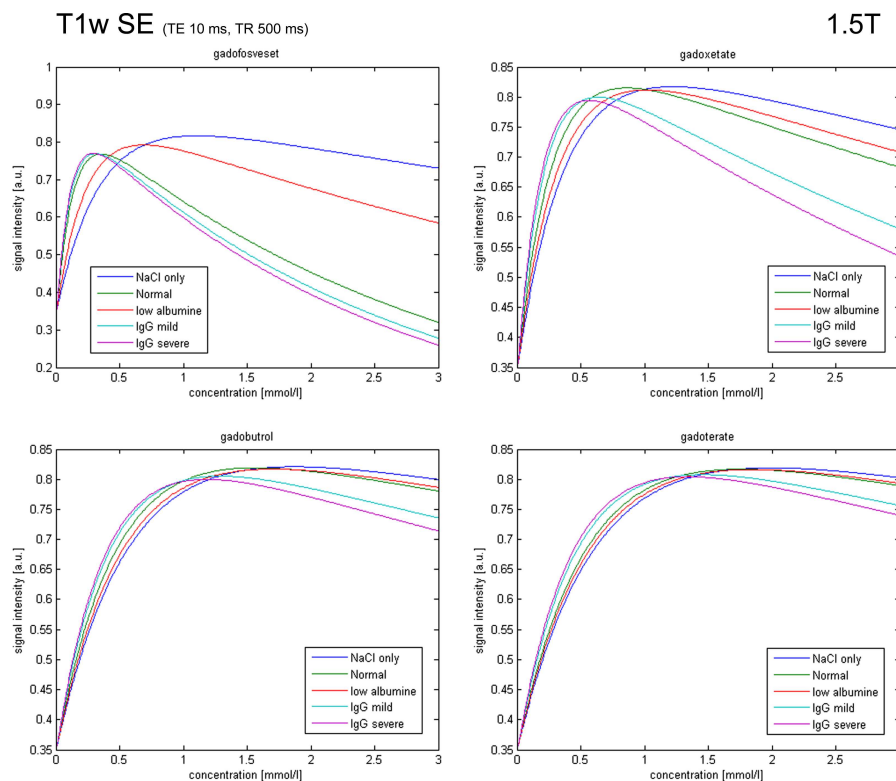


FIGURE 8. Simulated T1-weighted spin-echo signal as a function of contrast-medium and human serum-protein concentrations (TR/TE, 500 milliseconds/10 milliseconds; precontrast (tissue) T1/T2, 1000 milliseconds/100 milliseconds).

gadoxetate-induced MR signal changes strongly depended on both albumin and IgG concentration levels. For MR angiography, the most robust signal enhancement with the smallest protein-induced variation was projected for gadobutrol and gadoterate. The T2-weighted signal decrease to be expected in, for example, dynamic susceptibility-weighted imaging noticeably depended upon protein concentrations for all evaluated contrast agents.

DISCUSSION

The present investigation demonstrates that common pathological deviations from normal blood-serum protein concentration levels alter the signal enhancement induced by gadolinium-based MR contrast agents. Protein-level deviations of an extent that may be found in daily clinical practice in patients with liver failure, chronic inflammation, or multiple myeloma¹⁴ caused large changes of the relaxation rates of our test solutions, that of the contrast-agent relaxivities, and that of the projected MR imaging signal intensities.

An albumin deficiency decreased the relaxivities of all contrast agents, with gadofosveset showing the largest relative reduction. In contrast, the pathological elevation of IgG levels increased the relaxivities of all contrast agents, with gadoxetate showing the largest relative increase. The results translate into signal-intensity changes in contrast-enhanced MR imaging that, however, strongly depend on the type of the acquisition sequence, the field strength, as well as the type and concentration of the contrast agent.

Our study demonstrates significant effects of pathological IgG protein levels on contrast-agent relaxivities and quantifies contrast-agent-mediated as well as direct effects of albumin and IgG on water-proton relaxation rates. Equation [2] represents the simplest

model capable of summarizing and repredicting our experimental data by accounting for a direct influence of each protein on pre-contrast native relaxation rates and on contrast-agent relaxivity. Protein-contrast agent interactions have been modeled with more sophisticated equations before, for example, in the studies of Caravan⁸ or Henrotte.¹⁵ However, those require information or assumptions on the contrast-agent protein interaction, for example, the number of independent interaction sites, and could not reproduce the obvious influence on the transverse pre-contrast relaxation rates that albumin and, in particular, IgG exerted in our study. Equation [2] still assumes the relaxation enhancement to linearly grow with contrast-agent concentration. As Figures 4 and 5 demonstrate, this is a somewhat crude model for the observed transverse relaxation-rate enhancement, whereas it seems mostly satisfactory for the description of the longitudinal relaxation-rate enhancement.

It is well established that molar contrast-agent relaxivity increases with protein content.^{2,5,16,17} In the current study, IgG produced even larger effects per mass concentration, at least at 1.5 T, than albumin did, except for the contrast agent that specifically binds to albumin (gadofosveset). Proteins are believed to exert their influence by a slowing down of molecular reorientation of water and contrast-agent molecules and an increase in their orientational correlation times. Underlying mechanisms are a protein-induced increase in overall solution viscosity,^{6,18} an increased “microviscosity” in the protein hydration sphere, or a transient binding of the small molecules with corresponding temporary slowdown of their molecular tumbling.^{19,20}

In the absence of detailed knowledge about specific interactions and about 3-dimensional protein structure and accessible surface area, one could expect larger proteins with longer molecular

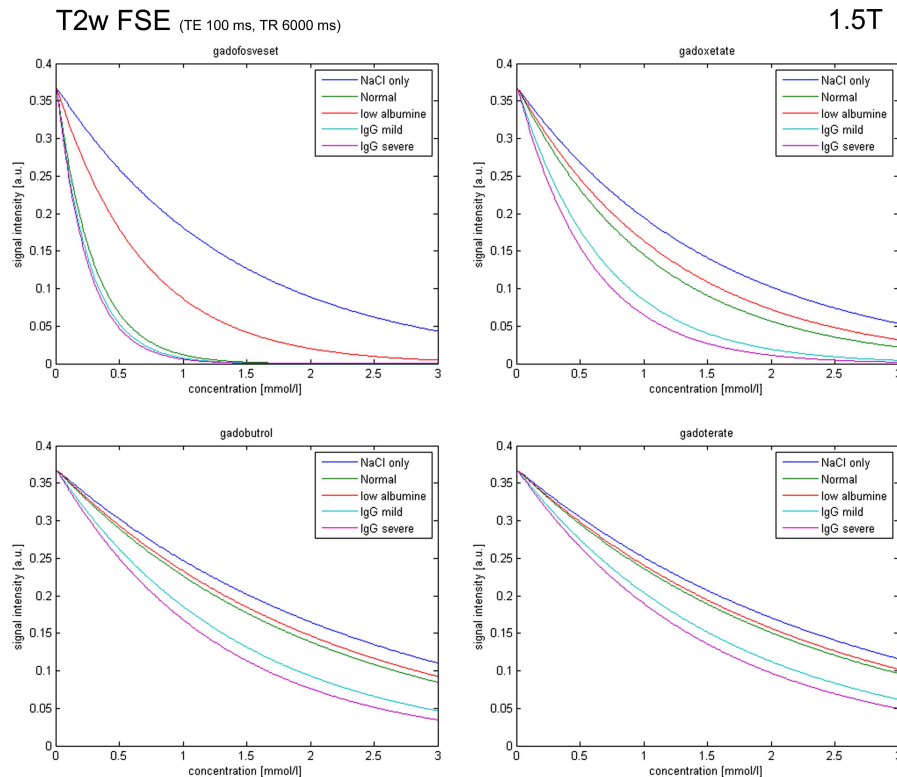


FIGURE 9. Simulated T2-weighted spin-echo signal as a function of contrast-medium and human serum-protein concentrations (TR/TE, 6000 milliseconds/100 milliseconds; precontrast (tissue) T1/T2, 1000 milliseconds/100 milliseconds).

reorientation times to exert a stronger influence because of a higher increase in time-averaged molecular re-orientation times of transiently bound smaller molecules.^{8,21} Because the IgG molecular mass (approximately 150 kDa) is approximately 3 times as large as that of albumin (67.5 kDa),²² IgG could, in agreement with our results, be expected to exhibit larger effects on contrast-agent relaxivities than albumin under the assumption of a non-specific weak binding and an equal number of binding sites per protein mass. The effect size of a smaller protein could reach or even surpass that of a non-specifically binding larger protein if it offered a particular contrast agent one or more tailored binding sites with optimally positioned protein functional groups that strongly increase either polar or non-polar attraction forces. This may well apply to the gadofosveset/albumin interaction and the corresponding large effects on water-proton relaxation. In the light of this tentative explanation of our results, even stronger effects, at least on transverse relaxivities, could be expected for proteins that are significantly larger than IgG, for example, immunoglobulin M.

It is not immediately clear how our *in vitro* results translate to clinical *in vivo* imaging. Considering the strong effects, it seems likely that, even in daily clinical practice, there will be a combination of imaging protocol, pathology, and data evaluation, where deviations from physiological protein concentrations noticeably distort the results. Assessment of parenchymal tissue perfusion based on increased R_2 relaxation rates during contrast-medium first pass, where signal changes are quantitatively converted to contrast-agent concentrations, may be a prime candidate for observation of such effects, compare Figure 10, particularly when standardized arterial input functions are used. Moreover, the protein-binding contrast agents exhibit a different clearance behavior with significant excretion from the liver compared with the predominant renal clearance of the

non-protein-binding contrast agents. If MR imaging is performed with a significant delay after bolus injection, the different clearance mechanisms may contribute to signal variations because of different plasma concentration levels besides influencing extravasation and, secondarily, also relaxivities in the interstitium according to local protein concentrations.

Our study has the following limitations:

- (a) Our solutions did not contain proteins of the $\alpha 1$, $\alpha 2$, and β -fractions of a normal serum protein electrophoresis because we could not obtain sufficient quantities of purified solutions. The $\alpha 1$ - and $\alpha 2$ -fractions, which contain most of the acute-phase proteins, and the β -fraction represent 1% to 4%, 7% to 13%, and 7% to 13% of total protein under physiological conditions, respectively, whereas γ -globulins constitute 8% to 16% and albumin constitute as much as 58% to 72%. Our protein solutions did not contain other abundant immunoglobulin classes normally present in serum either, such as immunoglobulin A and immunoglobulin M. Immunoglobulin G is, however, the most abundant one, with a serum concentration of 7 to 16 g/L, whereas IgA and IgM serum concentrations are 0.7 to 4.0 g/L and 0.4 to 2.3 g/L, respectively. Nevertheless, the previously mentioned missing proteins may interact stronger with contrast agents than do albumin and IgG.

As can be seen from the electrophoresis densitograms, the serum-protein profiles of our solutions resembled those of polyclonal gammopathies, as found, for example, in the case of chronic inflammation. Monoclonal gammopathies, as found in monoclonal gammopathy of undefined origin or multiple myeloma, give rise to a sharp, well-defined band, often within the γ -globulin fraction. The overexpressed immunoglobulin molecule could possibly interact stronger than IgG does in the current study.

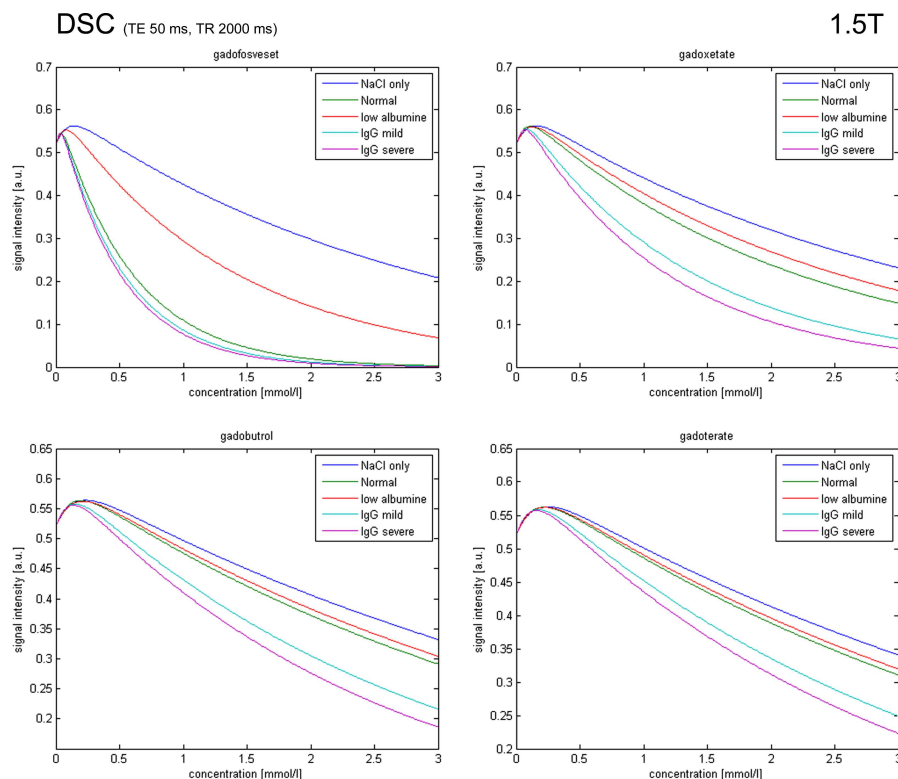


FIGURE 10. Simulated dynamic susceptibility-weighted MR imaging signal as a function of contrast-medium and human serum-protein concentrations (TR/TE, 2000/50 milliseconds; precontrast (tissue) T1/T2, 1000/100 milliseconds).

- (b) Because of restrictions of MR scanner software and the overall feasibility of the study, not all sequence parameters could optimally be set. Specifically, the TR of 6000 milliseconds was too short to allow full magnetization recovery in the T_1 measurements, and it was not increased with increasing TI. The minimum TI was limited to 50 milliseconds. Systematic errors may have resulted, for example, the slightly larger r_1 relaxivities at lower field strength for the dilution series with low and zero protein concentrations. Also, in the T_2 determination, for practicability reasons, the number of TEs was limited to 6. Finally, we measured up to 36 vials simultaneously without explicit correction of B1-field inhomogeneity. We believe that none of these had a major impact on the overall results of reported protein-induced relaxivity changes.
- (c) Because we could only include a small number of albumin (2) and IgG (3) concentrations in our study, we cannot exclude that non-linear dependencies or more complicated interaction models may need to be taken into account if more concentrations within the pathologic range could be evaluated. However, our results appeared rather stable in repeated evaluations with varying fit parameters and showed clear and logical trends, largely in agreement with previous literature reports, where such were available.
- (d) We worked with “molar” gadolinium concentrations, in moles gadolinium per liter solution, as opposed to molal (moles gadolinium per kilogram solvent) contrast-agent concentrations. Our primary focus was projected MR signal changes from a given volume (voxel) with a given amount of gadolinium upon pathological protein-content change. In this context, molar concentrations were of a more direct interest and allowed a more direct comparison with most previous studies comparing “molar” relaxivity data of multiple

contrast agents. For a study of the interactions of protein, contrast agent and water on a molecular level and molal concentrations would be advantageous. Such a detailed analysis was beyond the scope of our phenomenological study.

- (e) Because of constraints of measurement time, we were not able to completely compensate for all Gibbs ringing effects in the images, which, in principle, could have been compensated by higher spatial resolution and subsequently longer acquisition time.

This study has been published in parts as a conference abstract.²³

In conclusion, deviations of plasma-protein concentrations in aqueous solutions from physiological to pathological ranges result in significant changes of effective contrast agent relaxivities and may significantly alter the signal behavior of commonly applied MR imaging sequences.

REFERENCES

- Bellin MF, Van Der Molen AJ. Extracellular gadolinium-based contrast media: an overview. *Eur J Radiol.* 2008;66:160–167.
- Rohrer M, Bauer H, Mintorovitch J, et al. Comparison of magnetic properties of MRI contrast media solutions at different magnetic field strengths. *Invest Radiol.* 2005;40:715–724.
- Lauffer RB. Targeted relaxation enhancement agents for MRI. *Magn Reson Med.* 1991;22:339–342.
- Stanisz GJ, Henkelman RM. Gd-DTPA relaxivity depends on macromolecular content. *Magn Reson Med.* 2000;44:665–667.
- Giesel FL, von Tengg-Kobligh H, Wilkinson ID, et al. Influence of human serum albumin on longitudinal and transverse relaxation rates (r_1 and r_2) of magnetic resonance contrast agents. *Invest Radiol.* 2006;41:222–228.
- Wang Y, Spiller M, Caravan P. Evidence for weak protein binding of commercial extracellular gadolinium contrast agents. *Magn Reson Med.* 2010;63: 609–616.

7. Caravan P, Cloutier NJ, Greenfield MT, et al. The interaction of MS-325 with human serum albumin and its effect on proton relaxation rates. *J Am Chem Soc.* 2002;124:3152–3162.
8. Caravan P. Protein-targeted gadolinium-based magnetic resonance imaging (MRI) contrast agents: design and mechanism of action. *Acc Chem Res.* 2009;42:851–862.
9. Fasano M, Curry S, Terreno E, et al. The extraordinary ligand binding properties of human serum albumin. *IUBMB Life.* 2005;57:787–796.
10. Gornall AG, Bardawill CJ, David MM. Determination of serum proteins by means of the biuret reaction. *J Biol Chem.* 1949;177:751–766.
11. Pedregosa F, Varoquaux G, Gramfort A, et al. Scikit-learn: machine learning in Python. *J Mach Learn Res.* 2011;12:2825–3280.
12. Stanisiz GJ, Odrobina EE, Pun J, et al. T1, T2 relaxation and magnetization transfer in tissue at 3T. *Magn Reson Med.* 2005;54:507–512.
13. DiCiccio TJ, Efron B. Bootstrap confidence intervals. *Stat Sci.* 1996;11:189–212.
14. Vavricka SR, Burri E, Beglinger C, et al. Serum protein electrophoresis: an underused but very useful test. *Digestion.* 2009;79:203–210.
15. Henrotte V, Vander Elst L, Laurent S, et al. Comprehensive investigation of the non-covalent binding of MRI contrast agents with human serum albumin. *J Biol Inorg Chem.* 2007;12:929–937.
16. Pintaske J, Martirosian P, Graf H, et al. Relaxivity of gadopentetate dimeglumine (Magnevist), gadobutrol (Gadovist), and gadobenate dimeglumine (MultiHance) in human blood plasma at 0.2, 1.5, and 3 tesla. *Invest Radiol.* 2006;41:213–221.
17. Noebauer-Huhmann IM, Szomolanyi P, Juras V, et al. Gadolinium-based magnetic resonance contrast agents at 7 tesla: in vitro T1 relaxivities in human blood plasma. *Invest Radiol.* 2010;45:554–558.
18. Laurent S, Elst LV, Muller RN. Comparative study of the physicochemical properties of six clinical low molecular weight gadolinium contrast agents. *Contrast Media Mol Imaging.* 2006;1:128–137.
19. Adzamlı K, Vander Elst L, Laurent S, et al. Deuterium NMR study of the MP-2269: albumin interaction—a step forward to the dynamics of non-covalent binding. *MAGMA.* 2001;12:92–95.
20. Vander Elst L, Laurent S, Binto HM, et al. Albumin-bound MRI contrast agents: the dilemma of the rotational correlation time. *MAGMA.* 2001;12:135–140.
21. Aragon SR. Recent advances in macromolecular hydrodynamic modeling. *Methods.* 2011;54:101–114.
22. Kratz F, Elsadek B. Clinical impact of serum proteins on drug delivery. *J Control Release.* 2012;161:429–445.
23. Nanz D, Götschi S, Froehlich JM, et al. On contrast-enhanced MR imaging in the presence of pathological plasma-protein concentrations [abstract]. *ISMRM.* 2014. Abstract 558.